A New Astrophysical Setting for Chondrule Formation

Alexander N. Krot,[1*] Anders Meibom,[2] Sara S. Russell,[3] Conel M. O'D. Alexander,[4] Timothy E. Jeffries,[3] Klaus Keil[1]

Chondrules in the metal-rich meteorites Hammadah al Hamra 237 and QUE 94411 have recorded highly energetic thermal events that resulted in complete vaporization of a dusty region of the solar nebula (dust/gas ratio of about 10 to 50 times solar). These chondrules formed under oxidizing conditions before condensation of iron-nickel metal, at temperatures greater than or equal to 1500 K, and were isolated from the cooling gas before condensation of moderately volatile elements such as manganese, sodium, potassium, and sulfur. This astrophysical environment is fundamentally different from conventional models for chondrule formation by localized, brief, repetitive heating events that resulted in incomplete melting of solid precursors initially residing at ambient temperatures below approximately 650 K.

Chondrules are submillimeter-sized, rounded objects composed mainly of ferromagnesian silicates with accessory FeNi metal and minor sulfides. They are a major constituent of primitive meteorites called chondrites. Although the mineralogy, bulk chemistry, and textural properties of typical chondrules provide constraints on their formation, the exact mechanism of chondrule formation remains enigmatic (*1–4*). Typical chondrules (FeO-poor, or type I, and FeO-rich, or type II) show igneous, porphyritic textures, with phenocrysts of olivine and low-Ca pyroxene set in glassy mesostasis. These textures are consistent with crystal growth from a rapidly cooling (100 to 1000 K $hour^{-1}$) silicate melt (*5*). Chondrules often contain relic fragments of earlier generations of chondrules, suggesting that the chondrule-forming process was repetitive (*6–10*). Chondrule bulk compositions are generally very similar to CI (Ivuna-type) chondrites with the exception of the most volatile lithophile elements, such as Na, K, and S, which may have been lost during chondrule formation (*11–13*). Furthermore, chondrules in most chondrites are surrounded by fine-grained rims. On the basis of these observations, it is generally believed that chondrules formed in dusty regions of the solar nebula during localized, brief, repetitive heating events with peak temperatures of ~1800 to 2100 K. This resulted in incomplete melting of solid precursors initially residing at ambient temperatures below ~650 K, which is the condensation temperature of S (*3*). Shock waves (*14, 15*) and lightning discharges (*16, 17*) are currently favored as the most plausible chondrule-forming heating mechanisms (*18*).

[1]Hawai'i Institute of Geophysics and Planetology (HIGP), School of Ocean and Earth Science and Technology (SOEST), University of Hawai'i at Manoa, Honolulu, HI 96822, USA. [2]Geological and Environmental Sciences, 320 Lomita Mall, Stanford University, Stanford, CA 94305–2115, USA. [3]Department of Mineralogy, The Natural History Museum, Cromwell Road, London, SW7 5BD, UK. [4]Department of Terrestrial Magnetism, Carnegie Institution of Washington, 5241 Broad Branch Road NW, Washington, DC 20015, USA.

*To whom correspondence should be addressed. E-mail: sasha@pgd.hawaii.edu

Using optical and scanning electron microscopy, electron microprobe and ion microprobe analyses, and laser ablation inductively coupled plasma mass spectrometry (LA-ICP-MS) (*19*), we studied chondrules in two recently recovered meteorites: Hammadah al Hamra 237 (HH 237) and QUE 94411 (QUE). HH 237 and QUE are metal-rich chondrites and are probably genetically related to CR (Renazzo-type) and CH (high-metal carbonaceous) chondrites (*20, 21*). They are characterized by a high content of FeNi metal [~70 volume % (vol %); Fig. 1A], abundant chondrules (~30 vol %; Fig. 1B), relatively rare refractory inclusions (<1 vol %), and very rare clasts of fine-grained, heavily hydrated CI chondrite–like material. The chondrules and refractory inclusions show no evidence for aqueous alteration (*20–24*). Their bulk compositions show large depletions in moderately volatile lithophile and siderophile elements, which correlate with their volatility. On the basis of the presence of metastable FeNi metal grains, it was concluded that these meteorites escaped thermal metamorphism above ~500 K (*25*). Therefore, the volatility-related abundance patterns were established in the nebula before formation of these meteorites' parent body (*26, 27*). Their primitive nature makes these chondrites important for understanding high-temperature nebula processes that resulted in formation of their components.

HH 237 and QUE contain abundant FeNi metal grains (~20 vol %; Fig. 1A) that are zoned in major elements (Fe, Ni), minor elements (Co, Cr), and trace, platinum group elements (PGEs: Re, Os, Ir, Ru, Pt, Rh) (*25, 28, 29*). Their composition is consistent with an origin by fractional gas-solid condensation in the temperature interval from ~1500 to 1400 K, in a solar nebula region with a high initial dust/gas ratio (~10 to 50× solar) (*30, 31*), which experienced complete vaporization and relatively slow cooling (~1 to 5 K $hour^{-1}$) (*32*). On the basis of these slow cooling rates, the size of the formation region was estimated to be several million kilometers (*25*), which is inconsistent with the flash-heating events conventionally inferred for chondrule formation (*3*). The zoned metal grains are highly depleted in moderately volatile elements (Cu, Ga, Ge, As, Sn, S), requiring that, if these volatiles were present, the grains were isolated from the cooling nebula gas at high ambient temperatures (~1200 K) before volatile element condensation (*33, 34*).

Chondrules in HH 237 and QUE have no fine-grained matrix rims, contain no FeNi metal or sulfide, and can be divided into two textural types: skeletal olivine (SO) and cryptocrystalline (CC). Chondrules with porphyritic textures are absent (Fig. 2). There is a continuous transition between the SO and CC textural end-members (Fig. 1B). SO chondrules, or fragments thereof, are generally larger than CC chondrules; 25 to 250 μm versus 20 to 100 μm, respectively.

Both textural types of chondrules are Mg-rich and contain ~1 to 4 weight % (wt %) FeO and high Cr_2O_3 (0.5 to 0.9 wt %). SO chondrules consist of: (i) forsteritic olivine (Mg_2SiO_4) with a fayalite (Fe_2SiO_4; Fa) content of Fa_{2-4} and 0.2 to 0.6 wt % Cr_2O_3, (ii) Cr- and Al-bearing low-Ca pyroxenes with ferrosilite ($FeSiO_3$; Fs) and wollastonite ($CaSiO_3$; Wo) contents of $Fs_{1-5}Wo_{4-7}$ and (in wt %) 0.5 to 0.9 Cr_2O_3, 2 to 10 Al_2O_3, 0.2 to 0.5 TiO_2, (iii) high-Ca pyroxenes with Fs_{2-4}-Wo_{40-50} and (in wt %) 0.6 to 1.2 Cr_2O_3, 11 to 17 Al_2O_3, 0.7 to 1.4 TiO_2, and (iv) Na-free, Ca- and Al-rich glassy mesostasis. CC chondrules have pyroxene-olivine-normative compositions (Table 1). Individual minerals cannot be discerned in the CC chondrules, even at high magnification (×5000).

Chondrule bulk compositions normalized to Si and CI chondrites (*35*) show a continuum between SO and CC chondrules (Fig. 3A). SO and CC chondrules show large depletions in Mn, Na, and K (K content is below detection limit of the electron microprobe: <0.04 wt %). The SO chondrules, which are more refractory than CC chondrules, are enriched in refractory lithophile elements (Ca, Al, Ti) over CI levels, spanning the range from ~1.2 to 10× that of CI. Calcium, Al, and Ti abundance patterns are flat. The CC chondrules, which are less refractory, are depleted and complementary in these elements to SO chondrules and span the range from ~1 to <0.03× CI. The same relationship is observed for the rare earth

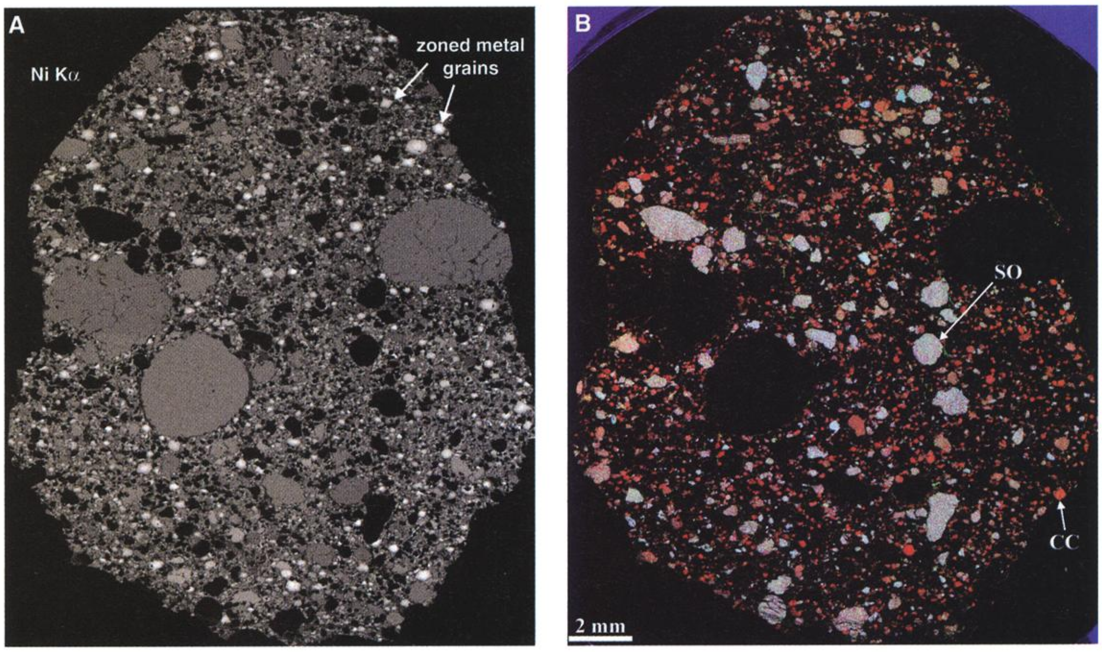

Fig. 1. (**A**) X-ray map in Ni Kα x-rays and (**B**) combined x-ray map composed of Mg Kα (red), Ca Kα (green), and Al Kα (blue) x-rays of Hammadah al Hamra 237. This metal-rich meteorite contains two types of chondrules: (i) large, Ca- and Al-rich chondrules (bluish) with SO textures, and (ii) small, Ca- and Al-poor chondrules (reddish) with CC textures. Most SO chondrules are fragmented. Chondrules contain no FeNi metal inclusions. About 20% of all FeNi metal grains are compositionally zoned with Ni-enriched cores.

elements (REEs), which also show flat abundance patterns (Fig. 3B). The CI-normalized REEs plot from ~1 to 10× CI for SO chondrules and from ~2 to <0.01× CI for CC chondrules.

The complementary behavior of refractory lithophile elements (Ca, Al, Ti, REEs) in SO and CC chondrules and the approximately solar bulk abundances of these elements in their host meteorites normalized to Mg and CI (*21, 36*) suggest that the SO and CC chondrules formed in a chemically closed system. The high Cr in chondrules and complementary depletions in FeNi metal (*21, 31, 36*) also suggest formation in a closed system. Assuming a solar composition for their formation region, the observed depletion of chondrules and metal in moderately volatile elements requires formation of both at high ambient temperature, above the condensation of these elements (*37*). Chondrules in HH 237 and QUE are metal-free (Fig. 1A), whereas silicate inclusions, texturally and compositionally similar to CC chondrules (*38*), are commonly observed inside chemically zoned FeNi metal condensates (Fig. 2, C and D). On the basis of these observations, we infer that chondrules formed in the same nebula region as zoned FeNi metal grains, but above the metal condensation temperature (~1500 K). The presence of 1 to 4 wt % FeO in chondrule silicates suggests that the chondrules or chondrule precursors formed under relatively oxidizing conditions, consistent with complete evaporation of a nebula region with enhanced dust/gas ratio of ~10 to 50× solar (*28, 39*). Similar dust/gas ratios are also inferred from the zoned FeNi metal grains (*28, 31*).

The absence of fine-grained rims and chondrules with porphyritic or granular textures suggests that chondrules in HH 237 and QUE crystallized in a dust-free environment from melts completely free of nuclei (*40*). The absence of dust is consistent with the conclusion, derived from the PGE distributions in zoned FeNi metal grains, that initially all solids were vaporized. This requires sustained temperatures in excess of ~1800 K (*29*).

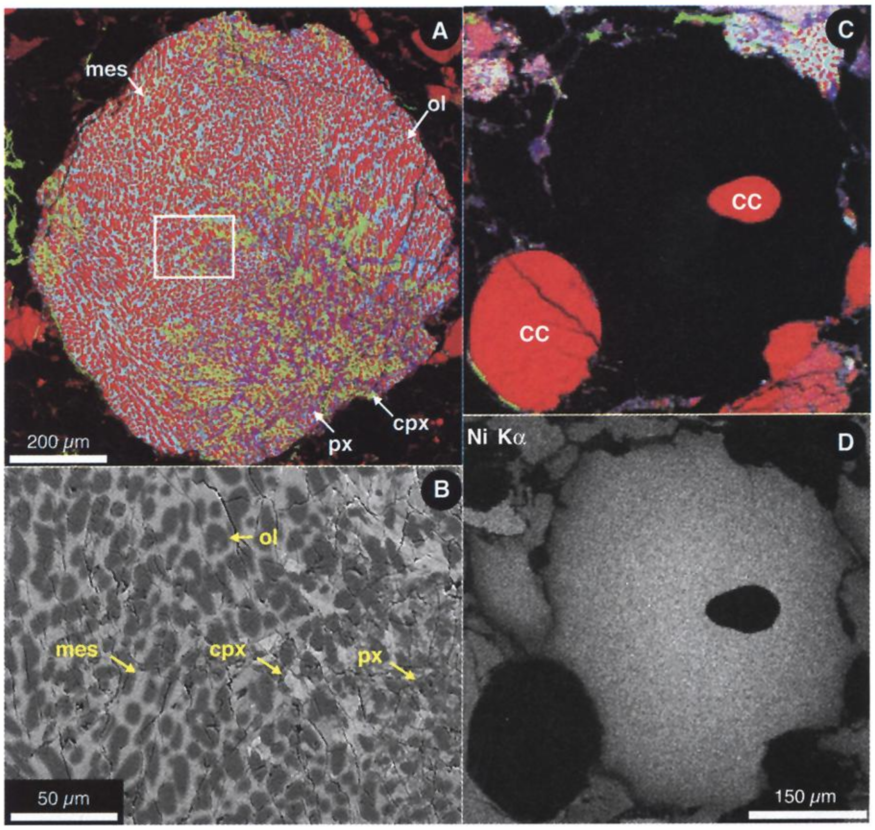

Fig. 2. (**A** and **C**) Combined x-ray maps composed of Mg Kα (red), Ca Kα (green), and Al Kα (blue) x-rays. (**B**) Backscattered electron image of inset in (A). (**D**) Ni Kα x-ray map. (A and B) SO chondrule composed of olivine (ol), high-Ca pyroxene (cpx), low-Ca pyroxene (px), and glassy mesostasis (mes). (C and D) Zoned metal grain enclosing and bordering cryptocrystalline chondrules (CC).

Two formation scenarios for the SO and CC chondrules can be considered. Either these chondrules formed by direct gas-liquid condensation or by prolonged heating of the gas-solid condensates above their liquidus temperatures, which destroyed all solid nuclei. In both scenarios, chondrule formation must have taken place at high temperatures before metal condensation. The inferred enhanced initial dust/gas ratios favor a gas-liquid condensation scenario (*41*).

The observed continuous range of refractory lithophile element abundances (from ~10× CI to <0.01× CI) and flat element patterns (Fig. 3) are explained by fractional condensation of chondrules or chondrule precursors in a closed system. The refractory lithophile elements were preferentially sequestered in the earlier formed SO chondrules, and the CC chondrules formed at lower temperatures when the gas was increasingly depleted in these elements.

The depletion of chondrules in moderately volatile elements (Mn, Na, K, S, Cu, Zn, Ga) suggests that they were efficiently isolated from the hot nebula gas before condensation of these elements (*42*). This requires fast transport of chondrules into colder (<650 K) nebula regions, where accretion of the meteorites took place. The exact mechanism responsible for this remains elusive. The X-wind, which is capable of transporting chondrule-sized objects from the innermost regions of the solar nebula out to planetary distances, might have played an important role in this process (*32, 43, 44*).

In contrast to typical chondrules, those in HH 237 and QUE appear to have escaped remelting by repetitive flash-heating in a region with low ambient nebula temperatures. Such recycling would have caused melting and homogenization of the zoned FeNi metal grains, formation of metal-bearing chondrules, porphyritic textures, relic grains, and enrichment of chondrules in moderately volatile elements, which are not observed.

The energetic and dynamical astrophysical environment recorded by chondrules and zoned FeNi metal grains in HH 237 and QUE could indicate that these meteorites formed earlier than most chondrites when the protoplanetary disk was more active (*25, 45*). Dating of the formation of these meteorites and their components should be possible and will determine whether this is correct.

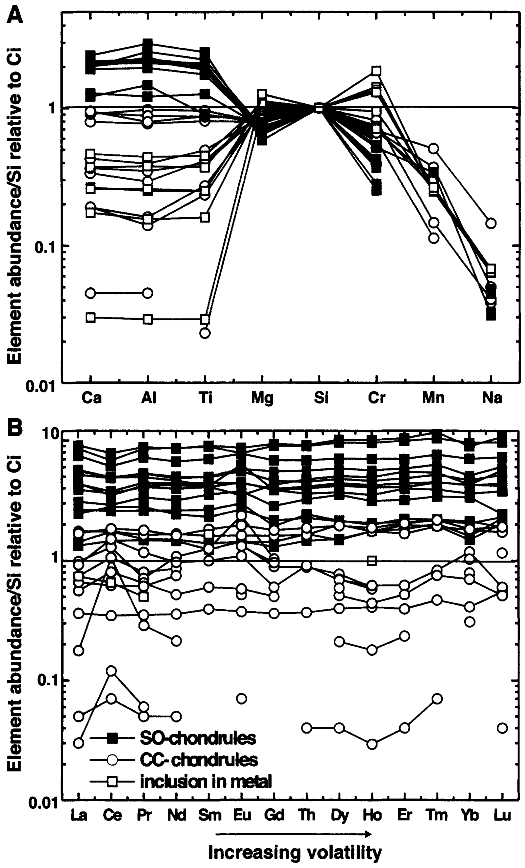

Fig. 3. (**A**) Bulk concentrations of major and minor lithophile elements and (**B**) REEs in SO and CC chondrules normalized to Si and CI chondrite abundances. In both diagrams, the SO and CC chondrules display complementarity. The SO chondrules are enriched in refractory lithophile elements (Ca, Al, Ti, REEs), and the CC chondrules are depleted in these elements relative to CI. All chondrules are highly depleted in the moderately volatile elements Mn and Na.

Table 1. Bulk compositions (in wt % normalized to 100%) of SO and CC chondrules.

Type	CC	CC*	CC	CC	CC	SO	SO	SO	SO
SiO_2	54.7	53.5	53.9	53.0	51.4	52.1	48.7	47.7	44.8
TiO_2	<0.04	<0.04	0.06	0.10	0.18	0.27	0.19	0.41	0.48
Al_2O_3	<0.05	0.08	0.77	1.9	3.8	5.8	7.0	11.0	12.2
Cr_2O_3	0.64	1.1	0.73	0.77	0.92	0.84	0.58	0.43	0.28
FeO	0.73	0.76	1.0	2.5	2.4	2.8	2.9	2.2	2.4
MnO	<0.07	0.14	<0.07	0.22	0.11	<0.07	0.25	<0.07	<0.07
MgO	43.8	44.4	42.8	39.9	37.6	33.4	35.9	30.5	32.5
CaO	<0.04	0.06	0.69	1.6	3.5	4.7	4.4	7.6	7.2
Na_2O	<0.05	<0.05	<0.05	<0.05	0.08	<0.05	0.06	0.06	0.09
K_2O	<0.04	<0.04	<0.04	<0.04	<0.04	<0.04	<0.04	<0.04	<0.04

*In chemically zoned FeNi metal grain; relative errors (1σ) are: SiO_2, Al_2O_3, MgO, and FeO, <3%; TiO_2, Cr_2O_3, MnO, and Na_2O, <1%.

References and Notes

1. R. H. Hewins, R. H. Jones, E. R. D. Scott, Eds., *Chondrules and the Protoplanetary Disk* (Cambridge Univ. Press, Cambridge, 1995).
2. R. H. Jones, T. Lee, H. C. Connolly Jr., S. G. Love, H. Shang, in *Protostars and Planets IV*, V. Mannings, A. P. Boss, S. S. Russell, Eds. (Univ. of Arizona Press, Tucson, AZ, 2000), pp. 927–963.
3. A. E. Rubin, *Earth Sci. Rev.* **50**, 3 (2000).
4. H. C. Connolly Jr., S. G. Love, *Science* **280**, 62 (1998).
5. H. C. Connolly Jr., R. H. Hewins, in (*1*), pp. 129–137.
6. A. E. Rubin, A. N. Krot, in (*1*), pp. 173–180.
7. R. H. Jones, in (*1*), pp. 163–173.
8. Additional observations supporting the repetitive nature of chondrule formation include the presence of coarse-grained igneous rims around chondrules (*9*) and the existence of independent compound chondrules (*10*). None of these features are observed for chondrules in HH 237 and QUE.
9. A. N. Krot, J. T. Wasson, *Geochim. Cosmochim. Acta* **59**, 4951 (1995).
10. J. T. Wasson, A. N. Krot, M.-S. Lee, A. E. Rubin, *Geochim. Cosmochim. Acta* **59**, 1847 (1995).
11. C. M. O'D. Alexander, in (*1*), pp. 233–243.
12. J. N. Grossman, in (*1*), pp. 243–257.
13. C. M. O'D. Alexander *et al.*, *Meteorit. Planet. Sci.* **35**, 859 (2000).
14. S. J. Weidenschilling, F. Marzari, L. L. Hood, *Science* **279**, 681 (1998).
15. L. L. Hood, D. A. Kring, in (*1*), pp. 265–277.
16. S. J. Desch, J. N. Cuzzi, *Icarus* **143**, 87 (2000).
17. M. Horanyi, S. Robertson, in (*1*), pp. 303–311.
18. A. P. Boss, in (*1*), pp. 29–35.
19. Backscattered electron images were obtained with a Zeiss DSM-962 scanning electron microscope using a 15-kV accelerating voltage and 1- to 2-nA beam current. Electron probe microanalyses were performed with a Cameca SX-50 electron microprobe using a 15-kV accelerating voltage, 10- to 20-nA beam current, beam size of ~1 to 2 μm, and wavelength dispersive x-ray spectroscopy. For most elements, counting times on both peak and background were 30 s. Matrix effects were corrected using PAP procedures. In order to reduce Na loss due to the interaction of the electron beam with the sample, Na concentration was determined in the first 10 s of the analyses. Bulk compositions of chondrules were determined using defocused (~7 μm) beam analysis. Detection limits for electron microprobe analysis were (in wt %): SiO_2, 0.04; TiO_2, 0.04; Al_2O_3, 0.05; Cr_2O_3, 0.06; FeO, 0.09; MnO, 0.07; MgO, 0.03; CaO, 0.04; Na_2O, 0.05; and K_2O, 0.04. X-ray elemental maps with a resolution of ~5 to 10 μm per pixel were acquired using the Cameca microprobe at 15-kV accelerating voltage, 50- to 100-nA beam current, and ~1- to 2-μm beam size. Trace elements were

analyzed using a VG PlasmaQuad LA-ICP-MS, with a 213-nm laser, and using a Cameca ims 6f ion probe. For details, see C. M. O'D. Alexander [*Geochim. Cosmochim. Acta* **58**, 3451 (1994)].
20. M. K. Weisberg *et al.*, *Meteorit. Planet. Sci.* **33**, A166 (1998).
21. M. K. Weisberg *et al.*, *Meteorit. Planet. Sci.*, in press.
22. A. N. Krot *et al.*, *Lunar Planet. Sci.* **31**, #1499 (2000) [CD-ROM].
23. A. N. Krot *et al.*, *Lunar Planet. Sci.* **31**, #1448 (2000) [CD-ROM].
24. A. J. Greshake, A. N. Krot, A. Meibom, K. Keil, *Meteorit. Planet. Sci.* **35**, A65 (2000).
25. A. Meibom *et al.*, *Science* **288**, 839 (2000).
26. J. T. Wasson (personal communication) questioned the classification of metal-rich CH and Bencubbin-like (HH 237 and QUE) meteorites as primitive carbonaceous chondrites and suggested that their unusual mineralogical and chemical characteristics could have resulted from melting, vaporization, outgassing, condensation, and size-sorting in a cloud of impact ejecta on the CR parent asteroid. According to this hypothesis, Ca- and Al-rich inclusions (CAIs) in CH and Bencubbin-like chondrites either survived this impact event or were added later during regolith gardening together with "normal" chondrules of porphyritic textures. The latter scenario can be excluded, because such "normal" chondrules are absent in HH 237 and QUE. Furthermore, the observed differences in mineralogy and chemistry of CAIs in CR, CH, and Bencubbin-like meteorites exclude a common source from the CR parent asteroid (*27*).
27. A. N. Krot *et al.*, in preparation.
28. M. I. Petaev, A. Meibom, A. N. Krot, J. A. Wood, K. Keil, *Meteorit. Planet. Sci.* **36**, 93 (2001).
29. A. J. Campbell, M. Humayun, A. Meibom, A. N. Krot, K. Keil, *Geochim. Cosmochim. Acta* **65**, 163 (2001).
30. The term "dust" is defined as a solid phase containing all elements but H and noble gases in cosmic proportions, and the dust/gas ratio as the atomic Si/H ratio normalized to the solar Si/H ratio of 3.58×10^{-5}. Note that astrophysicists conventionally define the dust/gas ratio as the mass of the dust component divided by the mass of gas component. According to this definition, the solar dust/gas ratio is ~0.005. See also (*35*).
31. The zoned FeNi metal grains in HH 237 and QUE contain three to four times less Cr than does metal condensed from a gas of solar composition, suggesting condensation under relatively oxidizing conditions, which could have resulted from complete evaporation of a solar nebula region with enhanced dust/gas ratios of ~10 to 50× solar (*28*, *30*).
32. A. Meibom *et al.*, *Meteorit. Planet. Sci.* **35**, A107 (2000).
33. A. J. Campbell, M. Hymayun, M. K. Weisberg, *Meteorit. Planet. Sci.* **35**, A38 (2000).
34. G. F. Herzog *et al.*, *Meteorit. Planet. Sci.* **35**, A71 (2000).
35. E. Anders, N. Grevesse, *Geochim. Cosmochim. Acta* **53**, 197 (1989).
36. J. Zipfel, F. Wlotzka, B. Spettel, *Lunar Planet. Sci.* **29**, #1417 (1998) [CD-ROM].
37. R. H. Hewins, *Geochim. Cosmochim. Acta* **55**, 935 (1991).
38. Silicate inclusions inside chemically zoned FeNi metal grains are texturally and compositionally similar to the CC chondrules, but tend to have higher Cr_2O_3 (1.1 ± 0.5 wt %) as a result of mild redistribution of Cr between metal and enclosed silicates by solid-state diffusion at high temperatures during FeNi metal condensation.
39. A. N. Krot, B. Fegley Jr., H. Palme, K. Lodders, in (*2*), pp. 1019–1055.
40. H. C. Connolly Jr., R. H. Hewins, *Geochim. Cosmochim. Acta* **59**, 3231 (1995).
41. D. Ebel, L. Grossman, *Geochim. Cosmochim. Acta* **64**, 339 (2000).
42. S. S. Russell, A. N. Krot, A. Meibom, C. M. O'D. Alexander, T. E. Jeffries, *Meteorit. Planet. Sci.* **35**, A139 (2000).
43. F. H. Shu, H. Shang, T. Lee, *Science* **271**, 1545 (1997).
44. F. H. Shu, H. Shang, M. Gounelle, A. E. Glassgold, T. Lee, *Astrophys. J.*, in press.
45. D. S. Woolum, P. Cassen, *Meteorit. Planet. Sci.* **34**, 897 (1999).
46. Supported in part by NASA grants NAG 5-412 (K. Keil, principal investigator), NAG 5-4225 (C. M. O'D. Alexander, principal investigator), and OSS (A. N. Krot, principal investigator). We thank the Meteorite Working Group, the Smithsonian Institution, M. Weisberg, and J. Zipfel for supplying samples. F. Shu and an anonymous reviewer are thanked for constructive reviews that helped improve the manuscript. A.M. is grateful for support from the Danish Natural Science Research Council. This is HIGP publication 1134 and SOEST publication 5335.

8 December 2000; accepted 22 January 2001

High Geomagnetic Intensity During the Mid-Cretaceous from Thellier Analyses of Single Plagioclase Crystals

John A. Tarduno,* Rory D. Cottrell, Alexei V. Smirnov

Recent numerical simulations have yielded the most efficient geodynamo, having the largest dipole intensity when reversal frequency is low. Reliable paleointensity data are limited but heretofore have suggested that reversal frequency and paleointensity are decoupled. We report data from 56 Thellier-Thellier experiments on plagioclase crystals separated from basalts of the Rajmahal Traps (113 to 116 million years old) of India that formed during the Cretaceous Normal Polarity Superchron. These data suggest a time-averaged paleomagnetic dipole moment of $12.5 \pm 1.4 \times 10^{22}$ amperes per square meter, three times greater than mean Cenozoic and Early Cretaceous–Late Jurassic dipole moments when geomagnetic reversals were frequent. This result supports a correlation between intervals of low reversal frequency and high geomagnetic field strength.

If there is an inverse relationship between reversal rate and paleointensity (*1*, *2*), it should be most obvious during geomagnetic superchrons, times during which the field apparently remains in one polarity for tens of millions of years. In particular, intensities during the 37-million-year long Cretaceous Normal Polarity Superchron should be higher than those of the Cenozoic or pre–mid-Cretaceous. However, there are few paleointensity results for the mid-Cretaceous (*3–5*). Thellier-Thellier (*6*) experiments often fail on whole rock basalt samples because of alteration during the successive heating steps required by the method. Results from mid-Cretaceous rocks that pass reliability checks are often not sufficiently numerous to average secular variation at the collection site.

Recently we have developed an approach to measure paleointensity using single plagioclase crystals separated from basalts (*7*, *8*). These crystals are affected less by experimental alteration (*7*, *8*). Analyses of magnetic separates by transmission electron microscopy reveal that these crystals contain single to pseudo–single-domain inclusions (50 to 250 nm) (*7*). In a test of the method, Thellier-Thellier analyses of plagioclase crystals from a 1955 flow from Kilauea volcano, Hawaii, yielded paleointensity estimates that agreed within error with those derived from the relatively fresh whole rocks (*9*) and magnetic observatory data (*7*).

Department of Earth and Environmental Sciences, University of Rochester, Rochester, NY, 14627, USA.

*To whom correspondence should be addressed. E-mail: john@earth.rochester.edu

The potential of measuring plagioclase for paleointensity analysis is best seen in older rocks where clays are ubiquitous. In a study of a single lava flow from the mid-Cretaceous [113 to 116 million years ago (Ma)] Rajmahal Traps of eastern India (*10*), Cottrell and Tarduno (*8*) show that directional data from oriented plagioclase crystals match those from the whole rock. Thermal demagnetization and magnetic hysteresis properties suggest that the plagioclase crystals and whole rocks have a similar, titanomagnetite mineralogy. Magnetic inclusions in the crystals are equant to rectangular, 100 to 350 nm in length, and not strongly aligned within the crystals (as indicated by hysteresis properties measured at different crystal orientations).

Magnetic hysteresis data (*8*) also indicate that a fine-grained magnetic phase forms in the whole rocks as a result of Thellier-Thellier heatings. The source of this fine-grained material is thought to be the alteration of clay in the whole rock ground mass. This behavior is not seen in the plagioclase crystals. This difference is reflected in the quality of the paleointensity results and their absolute value. Data from whole rocks often fail to meet reliability criteria. They generally